ELSEVIER

Colloids and Surfaces
A: Physicochemical and Engineering Aspects 206 (2002) 393–400

COLLOIDS AND SURFACES A

www.elsevier.com/locate/colsurfa

Determination of pore size distributions using the Dual Site-Bond Model: experimental evidence

R.H. López [a], A.M. Vidales [a,*], G. Zgrablich [a], F. Rojas [b], I. Kornhauser [b], S. Cordero [b]

[a] *Departamento de Física y CONICET, Universidad Nacional de San Luis, 5700 San Luis, Argentina*
[b] *Depatramento de Química, Universidad Autónoma Metropolitana, Iztapalapa, Mexico 09340, D.F., Mexico*

Abstract

In previous papers, we have described a suitable method to obtain pore size distributions for voids and necks using the Dual Site-Bond Model (DSBM) and Monte Carlo simulations. This method basically consists in the determination of the corresponding size distributions by using adsorption–desorption hysteresis data. Void size frequency functions are featured from the ascending curve. From the descending curve, we obtain a characteristic pressure value that will give us, via a quasi-universal curve, information about the neck size distribution function. In this work, we use our method to predict, using experimental hysteresis loops, the size distributions of several mesoporous samples. Once these functions are determined, we simulate the adsorption–desorption isotherms on a simple cubic network of voids and necks whose radii are sampled from the obtained size distributions. Comparison with experimental data is performed, drawing out fruitful conclusions and future perspectives based on the simplicity and predictive capability of the method.

Keywords: Adsorption; Hysteresis; Characterization; Mesoporous solids; Pore distributions

1. Introduction

Adsorption–desorption experiments are used as a standard method for characterization of mesoporous materials. Due to its great practical importance, this subject still stands as an open problem presenting interesting theoretical challenges [1–8]. One of the main features that accounts for the behavior of a porous solid in either transport or adsorptive phenomena is the knowledge of its pore size distribution. Although it may seem to be a feasible aspect to obtain experimentally, it is not, and implies a great deal of speculations when any of the experimental methods available to that end is selected. Whatever the method, it will introduce assumptions that necessarily will affect the resulting distributions. These assumptions start when the model describing the porous space is developed and continue when simplifications are introduced to the corresponding model of the physical process occurring in it. To illustrate this point, let focus our attention on the gas adsorption–desorption occurring in a mesoporous solid.

* Corresponding author. Tel./fax: +54-2652-425-109.
E-mail address: avidales@unsl.edu.ar (A.M. Vidales).

0927-7757/02/$ - see front matter
PII: S0927-7757(02)00062-6

It is well known that the shape and extent of adsorption–desorption hysteresis loops (ADHL) are influenced by several characteristics of the porous space, i.e. the geometrical shape of the pores, their size distribution, the interconnectivity of the porous network among others. Thus, the attainment of the pore size distributions of the solid from ADHL is a problem presenting two principal aspects. The first one, as mention above, is that a model describing the properties of the medium must be given, and secondly, within the context of that model, a procedure to determine the pore size distribution from the experimental information provided by ADHL must be developed.

We have already overcome these two stages with interesting results that are discussed in detail in [1,19]. A third step would be related with the proof of the proposed method by testing its prediction capabilities, i.e. by simulating ADHL with the obtained pore size distributions and comparing them with their experimental counterparts. This is the aim of the present work.

Modeling of porous media has evolved along two different, but complementary, lines: continuum and discrete models. Continuum models, based on a continuous characteristic function, attaining the value 0 at an empty point and 1 at a solid point, has proven to be more adequate to study the flux of fluids through the medium [9–13]. On the other hand, discrete models, representing the porous space by a network of voids (sites) connected by throats (bonds), have demonstrated to be a powerful tool to study the percolation properties of the medium and those phenomena depending on its topological properties [3,5,6,8,14–16].

The discrete model, usually referred as the Dual Site-Bond Model (DSBM), introduced by Mayagoitia et al. [3] is the simplest one which takes into account spatial correlation among pore sizes. Solid structures with very different topologies can be generated through this model. It has been shown [14,15] that spatial correlation among pore sizes affect drastically percolation probabilities. It has already been shown how ADHL are affected by spatial correlations in more realistic 3-D simulation models of pore space [1]. In the present work, DSBM will be the method employed to describe the porous space.

As is well known [6], there has been a number of attempts to generate a method to completely determine the porous space size distribution from experimental data. Some of these methods only obtain the void distribution, neglecting the existence of necks. On the other hand, others get two distributions (one for each entity) but fails when these two distributions overlap. This is due to the absence of any consideration of the possible presence of size correlation in the pore space structure [8]. Thus, we may say that the problem of obtaining the site and bond size distributions from the analysis of ADHL has been solved so far only for non-correlated porous networks and in the extreme cases where the pore volume can be attributed either entirely to the sites or entirely to the bonds [6,17,18]. It seems that the hypothesis that the main pore volume resides in the sites, while the bonds only play a role in the interconnectivity effects is reasonable for a variety of porous solids [6]. For simplicity and to keep correspondence with preceding analysis, we will assume this hypothesis through all our simulations presented here.

Here, we simulate sorption isotherms by representing the porous solid through a 3-D cubic network where the porous space is represented by sites and bonds (voids and necks) whose sizes are sampled from two distributions, one for sites and one for bonds. Usually, the shape of this functions is chosen as a lognormal function. The behavior of the threshold pressure for the evaporation process suggests a method to determine the bond from experimental adsorption–desorption hysteresis curves. This can be achieved by studying the behavior of the threshold as a function of the separation between the site and bond distributions and their dispersions [1].

Using experimental ADHL data of our own, we will first obtain the site and bond size distributions for three different mesoporous solids, Second, we will build a 3-D site-bond network simulating the solid via the DSBM. Finally, ADHL will be simulated to perform the comparison with the original experimental ones.

The method used here results in an encouraging new alternative to better describe and obtain pore size distributions that proves to be more close to the real ones, as we will see after presenting our results.

We remark that the present study is suitable for disordered porous materials, where network effects are important in the histheresis loop. However this is not the only effect contributing to the histheresis. Another important contribution, which can be better studied in ordered or taylored porous solids, comes from the thermodynamical behavior of the fluid in the pore and the occurrence of metastable states in the condensation–evaporation process and has been intensively studied by other authors [22–25].

2. Porous space model

As mentioned above, we model our solid using the DSBM. In what follows, we present a short explanation of its main features. Details of our model can be found elsewhere [1,3,4,8,14–16].

Let $S(R)$ and $B(R)$ be the distribution functions associated with the site and bond size R, and $F_S(R)$ and $F_B(R)$ the corresponding probability density functions, such that

$$S(R) = \int_0^R F_S(R')\,\mathrm{d}R'; \qquad B(R) = \int_0^R F_B(R')\mathrm{d}R' \tag{1}$$

The way in which sites and bonds are connected to form the network is given by the joint probability density function, $F(R_S, R_B)$, of finding a site with size $R_S \in (R_S, R_S + \mathrm{d}R_S)$ connected to a bond with size $R_B \in (R_B, R_B + \mathrm{d}R_B)$. The two basic laws describing the DSBM are:

$$B(R) - S(R) \geq 0 \tag{2}$$

$$F(R_S, R_B) = 0 \quad \text{for } R_S < R_B \tag{3}$$

The second law is often called the *Construction Principle* (CP). It is a law of a local nature and expresses the fact that the size R_B of any bond cannot be bigger than that of the two connected sites. If the joint probability function is expressed as

$$F(R_S, R_B) = F_S(R_S)F_B(R_B)\Phi(R_S, R_B) \tag{4}$$

Then, the correlation function Φ carries the information about the site-bond assignation procedure in the network. If we denote by Ω the overlapping area between the site and bond probability density functions, the function Φ has the following properties: (i) $\Phi_{\Omega\to 0}(R_S, R_B) = 1, \ \forall R_S, R_B$, meaning that in this limit sites and bonds are distributed completely at random, and (ii) $\Phi_{\Omega\to 1}(R_S, R_B) \propto \delta(R_S - R_B), \ \forall R_S, R_B$, sites and bonds group together in macroscopic patches, each having a value of R. Then, the overlapping Ω is the fundamental parameter describing the topology of the network in this model.

This behavior also suggests that Ω must be related to some *correlation length* (which would be a physically more meaningful parameter), characteristic of the decay of the spatial correlation function defined as:

$$C(r) = \left\langle R_S(\vec{r}_0)R_S(\vec{r}_0 + \vec{r})\right\rangle = \left\langle R_B(\vec{r}_0)R_B(\vec{r}_0 + \vec{r})\right\rangle \tag{5}$$

In fact, it is expected that $C(r)$ decays approximately as $C(r) \approx \exp(-r/l_0)$ where l_0 is the correlation length (measured in lattice constants). Thus, $l_0 \to 0$ for $\Omega \to 0$ and $l_0 \to \infty$ for $\Omega \to 1$.

We employ here the method presented in [8,20] for the Monte Carlo generation of such networks and remit the reader to such references for a detailed explanation. In what follows, we resume it in very simple terms.

An initial network is prepared by sampling the values of R_S and R_B from the corresponding probability density functions F_S and F_B and distributing them completely at random on the lattice. This network will have the correct F_S and F_B but not the correct $\Phi(R_S, R_B)$, in particular the CP is not obeyed everywhere. Then a Markov chain of new states of the network is generated by choosing at random pairs of sites (or bonds) attempting to exchange them, the exchange is accepted if it does not violate the CP. It has been demonstrated [20] that this procedure leads finally to the equilibrium distribution for the network and that it does not suffer of the imperfections introduced by other methods (mainly anisotropy). Once a network with the desired properties has

been generated, ADHL can be simulated according to the model to be described in Section 3.

3. Simulation of ADHL

Concerning the adsorption–desorption process simulated on the above described network, Kelvin equation is applied for condensation and evaporation processes, taking also into account the previous adsorbed layers in the ascending curve. A convenient form to the Kelvin equation is:

$$\ln(P/P_0) = -2\gamma V_L/R_m RT \quad (6)$$

where P/P_0 is the relative pressure of the vapor in equilibrium with a meniscus having a mean radius of curvature R_m. P_0 is the saturation vapor pressure corresponding to $R_m = \infty$, γ is the surface tension, and V_L is the molar volume of the liquid. During capillary condensation, the pore walls are already covered with an adsorbed film of thickness t_a. Thus, capillary condensation actually occurs not directly in the pore but rather in the inner core, and the relation between R_p (pore radius) and R_m is $R_p = R_m + t_a$, assuming that the contact angle between the liquid and the solid surface is zero. The thickness of the adsorbed film can be estimated using a multilayer adsorption isotherm, such as that given by the Halsey equation [21],

$$t_a = t_0 \left[\frac{a}{\ln(P_0/P)}\right]^b \quad (7)$$

where t_0 is the thickness of a single layer of adsorbed gas in Angstroms and a and b are constants for the gas/solid system. As said above, we assume all pore volume is concentrated in sites, whereas necks do not possess a volume of their own. Thus, the filling of every void on the adsorption branch of the isotherm is determined only by the individual void characteristics and does not depend on the neck-size distribution. In particular, voids with radii lower than the Kelvin radius, $R < R_p$, are completely filled and those with $R > R_p$ are filled only partly via reversible sorption mechanism (multilayer adsorption). A differential analysis of the adsorption branch of the isotherm allows then the determination of the void-size distribution (site distributions).

The desorption process is dependent both on the void (site) and neck (bond) size distributions, $F_s(R)$ and $F_b(R)$. If the radii of all the voids are larger than those of all the necks, i.e. void and neck arrangements are random, the desorption process is mathematically equivalent to the bond problem in percolation theory. In practice, the case in which the size distributions of voids and necks do not overlap is rare. In general, these distributions may be overlapping, introducing correlations in the arrangement of voids and necks.

For the desorption stage, a pore (site or bond), having the appropriate radius ($R > R_p$), evaporates only if it is connected to the vapor phase by a continuous path of already evaporated pores. This last condition introduces cooperative effects in the desorption branch that are well known [1,4,5]. This *percolation* effect produces an inhibition of the evaporation process: the larger is the percolation threshold the greater will be the retarding on the evaporation branch.

In all our present simulations, ADHL are simulated on simple cubic porous networks of $50 \times 50 \times 50$. It is worth mentioning that finite size effects become negligible for L (linear size of the network) greater or equal to 50 lattice units. In order to generate the network, site and bond sizes were sampled from the distributions obtained following the method explained in Section 4. Once the desired porous network is ready, sorption isotherms are simulated as explained above, recording the adsorbed or desorbed volume V as a function of P/P_0 in order to compare the results with the corresponding experiments.

4. Determination of pore size distributions

Assume you have a complete set of data belonging to primary gas adsorption–desorption processes onto a mesoporous solid. As said above, one can determine the size distribution of sites from the adsorption branch of the isotherm. In [1] we proposed a method to determine the corresponding bond (neck) distribution using the fact that a quasi-universal behavior was found for the mean bond size (B_m) against relative pressure P^*,

where the later is the relative pressure at which the relative desorbed volume has a value of 0.9. The relation between B_m and P^* is plotted in Fig. 1 for different values of the mean size for sites, S_m, and the dispersion σ of the site distribution and is approximately given (in nanometers) by:

$$B_m = \frac{1}{1 - P^*} \tag{8}$$

We used this method to obtain the size distributions of one Vycor glass sample and a couple of silica samples with different active sites, i.e. SiO_2–Cu and SiO_2–DIOL whose experimental ADHL are of our own. In the case of the Vycor glass, the adsorbate was Xe and for the silica solids it was N_2. The procedure is basically as follows. Starting from experimental ADHL, we obtain each site size distribution from the adsorption branch of each sample. Different differential analysis were used and the distributions obtained little differ from one method to another. The resulting distributions are conveniently fitted with log-normal functions. Then, the value for S_m is determined. Using the desorption branch of each sample we get the value of P^*, i.e. the relative pressure at which the relative adsorbed volume was 0.9. Thus, with both S_m and P^*, we use the quasi-universal curve from Fig. 1 to set the value of B_m. To determine the bond distribution we assume a log-normal shape for it with a dispersion half the value of that corresponding to the site distribution. This choice is based on experimental evidence suggesting that neck distributions are always narrower that void ones [6,17]. The results for the corresponding size distribution for the three samples are shown in the insets of Figs. 2–4. As can be seen, the bond distributions are truncated for radii values smaller than the range of validity of Kelvin equation. Only the lines corresponding to the log-normal fitting functions are shown. These fitting functions are then used in the simulation program to obtain the porous solid that will represent each of the samples. After the networks are generated, we proceed by simulating the primary isotherms for gas sorption and compare the simulations with experimental results.

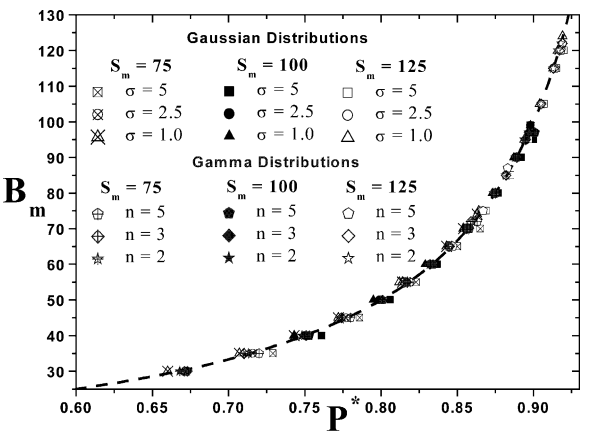

Fig. 1. Plot of the quasi-universal empirical relation between B_m and P^* showing the collapse of all the data on a single curve. The dashed line represents Eq. (8).

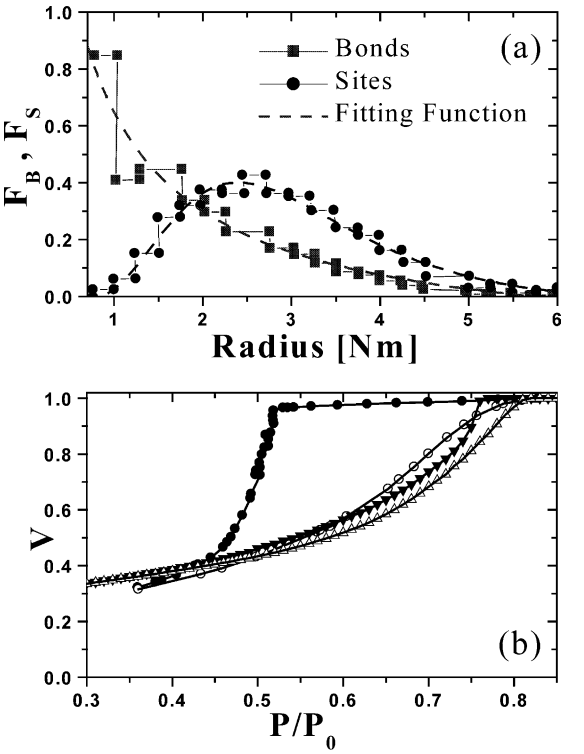

Fig. 2. (a) Site and bond normalized distribution functions obtained from a differential method (sites) and from the quasi-universal curve (bonds). (b) ADHL for Xe (at 151 K) on Vycor porous glass. Circles correspond to experimental data from [17] and triangles correspond to simulated isotherms using our method. Empty symbols correspond to adsorption and full ones to desorption.

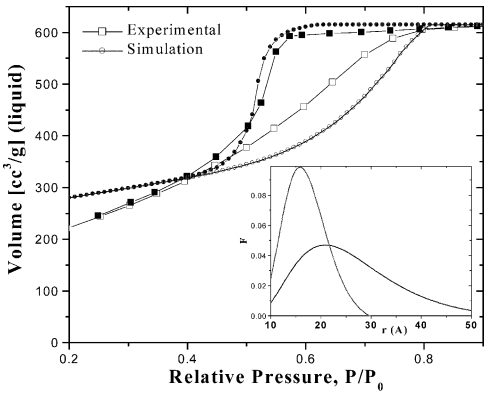

Fig. 3. Site and bond size density distribution functions obtained following our proposed method (inset) and the corresponding ADHL for N_2 (at 77 K) on SiO_2–Cu. Circles correspond to experimental data from our own and triangles correspond to simulated isotherms using our method. Empty symbols correspond to adsorption and full ones to desorption.

5. Experimental

Here we briefly review the experimental details for sample preparation and adsorption–desorption measurements. More details can be obtained from Ref. [17].

For the preparation of highly-mesoporous silica specimens for pure silica samples the sol–gel method was used. Tetraethyl-orthosilicate (TEOS) of analytical purity, was chosen as the silica precursor. The synthesis was performed in a glass round-bottom flask at room temperature (25 °C) by dissolving 37.9 cm^3 of TEOS in 59 cm^3 of ethanol under a gentle stirring during some minutes. Afterwards, the amount of water necessary for the hydrolysis reaction (12 cm^3) was added together with a mixture of hydrofluoric and hydrochloric acids, the stirring being kept for further 30 min. The sol was then taken out of the reactor and poured into glass cylinders where gelation eventually occurred. One of the silica monoliths was prepared with a diolic agent using the same amounts of the above reactants, but this time including 14 cm^3 extra of ethylene glycol that was added together with the TEOS–ethanol solution. Gels were dried in an oven at 100 °C for 48 h. The final xerogels were obtained as gelatinous but intact (no cracks) cylindrical mass that could be removed from the mould. The materials were calcined at 500 °C during 10 h to finally obtain rigid mesoporous silica monoliths.

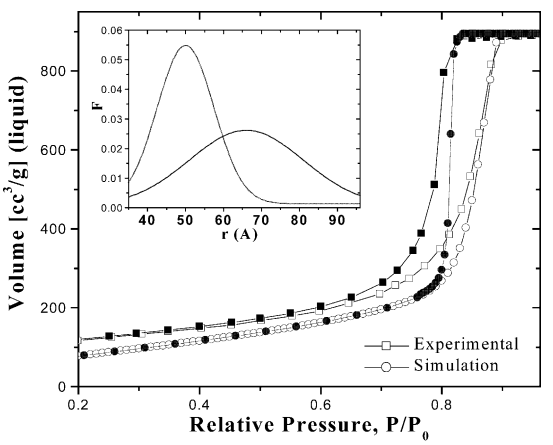

Fig. 4. Site and bond size density distribution functions obtained following our proposed method (inset) and the corresponding ADHL for N_2 (at 77 K) on SiO_2–DIOL. Circles correspond to experimental data from our own and triangles correspond to simulated isotherms using our method. Empty symbols correspond to adsorption and full ones to desorption.

In the case of doped silica samples, doped silica monoliths were synthesized in the same way as for pure silica specimens. In the case of SiO_2–Fe monoliths, the iron source was 1.3 g of $Fe(NO_3)_3 9H_2O$ that was introduced together with the water used for the reaction. For the SiO_2–Cu materials, the copper source was 0.56 g of $CuCl_2 \cdot 2H_2O$. The drying and calcinations procedures were the same as those employed for the pure silica substrata.

Adsorption–desorption isotherms were measured on the samples with an authomatic Quantachrome Autosorb-1-LC apparatus. Samples were outgassed at 300 °C for 10 h and stored under helium previously to the adsorption–desorption runs.

6. Results and discussion

In Figs. 2–4 we show the results of our simulated isotherms for the three solids mentioned above. In Fig. 2 we plot the obtained results for Vycor glass along with the experimental data from Ref. [17] from which we extract the experi-

mental ADHL. As clearly seen, the coincidence with experimental results is quite good given the simplicity of the method. The departure from the real isotherm is due mainly to two factors. The first one related to the assumption that all the volume space is concentrated in sites, thus, the volume added by condensation in bonds to the experimental adsorbed volume at a given relative pressure is not taken into account in the simulations. The second reason is due to the initial adsorbed volume in the multilayer region, i.e. the contribution to the total adsorbed volume made by the successive layers adsorbed on the pore walls up to the inception point. On one hand, this volume is not taken into account when the differential method is used. On the other hand, the volume we obtain in our simulations from the beginning of adsorption to the inception point, is only approximated because Eq. (7) is no longer valid in this region of multilayer adsorption. It is worth to mention that the bond distribution shown in Fig. 2(a) is not exactly centered at the B_m value obtained using the quasi-universal curve, in fact, it is a little bit lower than B_m. The reason of this change was to allow a smaller overlapping area between the two size distributions, in order to accelerate the generation algorithm of the porous solid given that, as the overlapping area increases, CPU time consuming increases critically. Thus, our prediction for the behavior of the desorption branch is that it will get closer to the experimental data given that percolation effects diminish with increasing overlap (increasing correlations) and, consequently, the position of the knee will move to the right in pressures and the loop will get a little narrower. This will improve the coincidence of simulations and experiment.

In Fig. 3 we plot the results for the SiO_2–Cu solid. The simulated branch does not follow its experimental counterpart. The reason for this disagreement may be attributed, as said above, to the assumptions made concerning the behavior in the multilayer region, Eq. (7). In previous works [1], we have performed adsorption isotherms with a different equation describing t_c and found that, for some solids, this branch may be very sensitive to the model. On the other hand, the simulated data describe closely the desorption behavior of the solid. The knee of the branch is in very good agreement with the experiment and the desorption slope is close to the expected behavior.

The second silica sample, SiO_2–DIOL, have a very different porous space. In fact, it is important to remark the great difference in the pore distributions of the two silica samples. As seen from the corresponding insets, the mean values for the site distributions differ in more than 30 Å, so do the bond distributions, too. Even though, the simulated ADHL obtained from the method describes correctly the shape of the loop, that, in fact, looks very different compared with the previous one. For this sample, the analysis of the coincidences and departures from experimental behavior are closely the same as the ones made for the first silica sample.

Both desorption knees agree quite well with the experimental data. This means that the expected percolation delay for solids with size correlation topology, like the ones studied here, is conveniently described by our method and it also seems to describe correctly hysteresis loops that differ considerably in shape.

We believe that another reason for the difficulties encountered in describing the adsorption branch, is the great sensitivity of the differential method employed to obtain the corresponding size distribution from steep experimental ascending curves.

The present method is simple and shows a very good qualitative description for ADHL. Its quantitative prediction capability is still unsatisfactory, but better than that of traditional methods [19]. Our present efforts are directed in improving this capability.

Acknowledgements

Authors want to thank finantial suport from Universidad Nacional de San Luis, CONICET and the Mexican–Argentinian contract CONACyT-SECyT in the context of the Proyect 'Complex Media and Physicochemistry of Surfaces' Universidad Autónoma de México.

References

[1] R.H. López, A.M. Vidales, G. Zgrablich, Langmuir 16 (2000) 6999 and references there in.
[2] S.J. Gregg, K.S.W. Sing, Adsorption, Surface Area and Porosity, Academic Press, New York, 1982.
[3] V. Mayagoitia, B. Gilot, F. Rojas, I. Kornhouser, J. Chem. Soc. Faraday Trans. I 84 (1988) 801.
[4] V. Mayagoitia, in: F. Rodriguez-Reinoso, J. Rouquerol, K.S. Sing, K.K. Unger (Eds.), Characterization of Porous Solids III, Elsevier, Amsterdam, 1991, p. 51.
[5] N.A. Seaton, Chem. Eng. Sci. 46 (1991) 1895.
[6] V.P. Zhdanov, Adv. Catal. 39 (1993) 1.
[7] C.M. Lastoskie, N. Quirke, K.E. Gubbins, in: W. Rudzinski, W.A. Steele, G. Zgrablich (Eds.), Equilibria and Dynamics of Gas Adsorption on Heterogeneous Solid Surfaces, Elsevier, Amsterdam, 1997, pp. 745–776.
[8] I. Kornhauser, R.J. Faccio, J.L. Riccardo, F. Rojas, A.M. Vidales, G. Zgrablich, Fractals 5 (1997) 355.
[9] M. Chaouche, N. Rakotomala, D. Salin, B. Xu, Y.C. Yortsos, Chem. Eng. Sci. 49 (1994) 2447.
[10] J. Sallés, J.F. Thovert, P.M. Adler, in: J. Rouquerol, F. Rodríguez-Reinoso, K.S.W. Sing, K.K. Unger (Eds.), Characterization of Porous Solids III, Elsevier, Amsterdam, 1994.
[11] M. Giona, A. Adrover, AIChE J. 42 (1996) 1407.
[12] A.P. Roberts, M.A. Knackstedt, Phys. Rev. E 54 (1996) 2331.
[13] D. Loggia, D. Salin, Y.C. Yortsos, Phys. Fluids 10 (1998) 747.
[14] R.J. Faccio, G. Zgrablich, V. Mayagoitia, J. Phys. C. Condens. Matter 5 (1993) 1823.
[15] A. Vidales, R. Faccio, J. Riccardo, E. Miranda, G. Zgrablich, Phys. A 218 (1995) 19.
[16] A.M. Vidales, R. López, G. Zgrablich, Langmuir 15 (1999) 5703.
[17] G. Mason, Proc. R. Soc. Lond. Ser. A 415 (1988) 453.
[18] M. Parlar, Y.C. Yortsos, J. Colloid Interface Sci. 132 (1989) 425.
[19] R.H. López, A.M. Vidales and G. Zgrablich, Pore Size Distribution Determination from Sorption Isotherms: Comparison with Traditional Methods, Proc. of the 7th International Conference on Fundamentals of Adsorption, Nagasaki, 20–25 May 2001, to be published.
[20] J.L. Riccardo, W.A. Steele, A.J. Ramirez, G. Zgrablich, Langmuir 13 (1997) 1064.
[21] G.D. Halsey, J. Chem. Phys. 16 (1948) 931.
[22] A.V. Neimark, A. Vishnyakov, Phys. Rev. E 62 (2000) 4611.
[23] A.V. Neimark, P.I. Ravikovitch, A. Vishnyakov, Phys. Rev. E 62 (2000) 1493.
[24] R. Evans, U.M.B. Marconi, P. Tarazona, J. Chem. Phys. 84 (1986) 2376.
[25] A. de Keizer, T. Michalski, G.H. Findenegg, Pure Appl. Chem. 10 (1991) 1495.